Original Article

Myogenic differentiation of human amniotic mesenchymal cells and its tissue repair capacity on volumetric muscle loss

Journal of Tissue Engineering
Volume 10: 1–13

DOI: 10.1177/2041731419887100
journals.sagepub.com/home/tej
SAGE

Di Zhang[1*], Kai Yan[1*], Jing Zhou[1*], Tianpeng Xu[1], Menglei Xu[1], Jiayi Lin[2], Jiaxiang Bai[2], Gaoran Ge[2], Dan Hu[1], Weibing Si[1], Yuefeng Hao[1] and Dechun Geng[2]

Abstract

Stem cell–based tissue engineering therapy is the most promising method for treating volumetric muscle loss. Human amniotic mesenchymal cells possess characteristics similar to those of embryonic stem cells. In this study, we verified the stem cell characteristics of human amniotic mesenchymal cells by the flow cytometry analysis, and osteogenic and adipogenic differentiation. Through induction with the DNA demethylating agent 5-azacytidine, human amniotic mesenchymal cells can undergo myogenic differentiation and express skeletal muscle cell–specific markers such as desmin and MyoD. The Wnt/β-catenin signaling pathway also plays an important role. After 5-azacytidine-induced human amniotic mesenchymal cells were implanted into rat tibialis anterior muscle with volumetric muscle loss, we observed increased angiogenesis and improved local tissue repair. We believe that human amniotic mesenchymal cells can serve as a potential source of cells for skeletal muscle tissue engineering.

Keywords

Human amniotic mesenchymal cells, myogenic differentiation, volumetric muscle loss, tissue engineering

Date received: 14 August 2019; accepted: 17 October 2019

Introduction

Skeletal muscle has a strong self-repair ability; it can completely restore itself when exposed to minor damage; but, when large muscle loss occurs, the skeletal muscle self-repair process will be hindered. Generally, muscle damage is known as volumetric muscle loss (VML) when the missing volume of the damaged muscle is 20% or more. At present, the treatment of VML in clinical practice is often limited to simple debridement closure or flap transplantation. These methods do not induce sufficient muscle tissue regeneration, and the outcome is often a large amount of fiber deposition and scar formation in the defect area, resulting in functional limitation or even permanent disability.[1,2]

In recent years, an increasing number of studies have been devoted to improving tissue regeneration and functional improvement after VML. The main methods used include autologous muscle grafting, microvascular fragment

[1]Orthopedics and Sports Medicine Center, The Affiliated Suzhou Hospital of Nanjing Medical University, Suzhou, People's Republic of China
[2]Department of Orthopedics, The First Affiliated Hospital of Soochow University, Suzhou, People's Republic of China

* Contribute equally to this work.

Corresponding authors:
Weibing Si, Orthopedics and Sports Medicine Center, The Affiliated Suzhou Hospital of Nanjing Medical University, Suzhou 215006, People's Republic of China.
Email: si_weibing@hotmail.com

Yuefeng Hao, Orthopedics and Sports Medicine Center, The Affiliated Suzhou Hospital of Nanjing Medical University, Suzhou 215006, People's Republic of China.
Email: 13913109339@163.com

Dechun Geng, Department of Orthopedics, The First Affiliated Hospital of Soochow University, Suzhou 215006, People's Republic of China.
Email: szgengdc@163.com

transplantation, acellular scaffold implantation, and cell therapy. Although autologous muscle grafting has produced the best enhancement of tissue regeneration and functional improvement,[3,4] the frequency of morbidity in donor sites is unacceptable. Microvascular fragment grafting[5,6] and acellular scaffold implantation[7,8] cannot induce sufficient tissue regeneration and can even aggravate fiber deposition. While cell therapy seems to show the most promise outcome, muscle and adipose-derived stem cells (ADSCs) were most widely used, but satellite cells[9] and ADSCs[10,11] used in previous studies were difficult to extract and shown poor histology.

The amniotic membrane has a wide variety of sources and is often treated as medical waste, eliminating ethical issues. Amniotic membrane has been used clinically for more than a century. It contains two types of cells: amniotic epithelial cells (AECs) and amniotic mesenchymal cells (AMCs). Research has confirmed that AMCs are pluripotent.[12,13] Previous research studies have shown that human amniotic mesenchymal cells (hAMCs) can increase bone strength and reduce fracture susceptibility by osteogenic differentiation and promoting endogenous osteogenesis,[14] and its cartilage repair capacity have been revealed[15] that hAMCs can also differentiate into anterior cruciate ligament fibroblasts[16] and even islet[17]; however, whether it could be used in skeletal muscle injury remained unclear. 5-Azacytidine (5-Aza) is an inhibitor of DNA methyltransferase; 5-Aza can induce pluripotent stem cells differentiate into the direction of myoblast cell lineages via changes in the methylation of DNA.[18,19] According to previous studies, human amniotic fluid cells can express the skeletal muscle cell–specific markers after exposure to 5-Aza,[20] and even in mouse embryonic stem cells lacking Pax7, which is an important factor for the differentiation of myogenic precursor cells, 5-Aza induction can still increase the expression of myogenic proteins.[21] In this study, we extracted hAMCs from placenta obtained from cesarean sections, examined their myogenic differentiation ability under the induction of 5-Aza, and explored their potential effect in VML repair.

Methods and materials

Isolation and culture of hAMCs

Placenta was obtained from cesarean sections of pregnant women who gave full-term birth (37–42 weeks of gestation) and women with intrauterine infection were excluded, all patients were provided with verbal informed consent. Our research was approved by the Ethics Committee of the First Affiliated Hospital of Soochow University (approval number: 201805A008), and the experiments followed the relevant ethical rules. Briefly, we obtained placental tissue by bluntly separating the fetal side of the placenta tissue with a vascular clamp under sterile conditions, and a piece of semitransparent amnion tissue approximately 10 cm × 10 cm in size was isolated and placed in a 50-mL centrifuge tube containing sterile phosphate-buffered saline (PBS). The tissue was brought into the laboratory and stored at 4°C, and cell extraction was performed within 6 h. The amniotic membrane was repeatedly washed with sterile PBS to remove blood clots and amniotic fluid and cut into fragments 1 mm × 1 mm in size, and 5% trypsin was used to remove human amniotic epithelial cells (hAECs) via incubation at 37°C for 10 min. After digestion, the tissue was filtered through a 200-mesh filter, and the filtrate was collected and centrifuged. The precipitate was resuspended in Dulbecco's Modified Eagle's (DME)/F12 complete medium (HyClone, Logan, Utah, USA) containing 1% penicillin and streptomycin supplemented with 10% fetal bovine serum (FBS) and maintained in an incubator at 37°C in 5% carbon dioxide. The remaining tissue fragments were washed twice with PBS, and 5% type II collagenase (C6885, Sigma, USA) was added to digest the tissue fragments in a 37°C water bath for 1 h, and the tissues were shaken once every 10 min until no obvious tissue fragments could be observed. The digestion was terminated by adding an equal volume of PBS, and the cell suspension was filtered using a 100-μm cell strainer to remove undigested tissue. Then, the filtrate was centrifuged at 1500 r/min for 10 min, the supernatant was discarded, and the precipitate was washed three times with PBS. Finally, the precipitate was suspended in DME/F12 complete medium containing 1% penicillin and streptomycin supplemented with 10% FBS in a 37°C incubator with 5% carbon dioxide. On the second day, the culture medium was changed, the exfoliated cells and tissue block were discarded, and the adherent cells were further cultured. On the 10th day, when the density of the cells reached approximately 80%, the cells were passaged at a ratio of 1/3, and the cells generated after P3 were used in experiments.

Flow cytometry analysis of the hAMCs

hAMCs (P4) were analyzed by flow cytometry using fluorescein isothiocyanate (FITC)-conjugated mouse anti-human CD34, CD45, CD73, CD90, CD105, and human leukocyte antigen—DR isotype (HLA-DR) antibodies (Biolegend, California, USA). The cells were incubated with antibody for 30 min at 4°C and assayed with a flow cytometer.

Multilineage differentiation potential of the hAMCs

In a 12-well plate, when the density of the hAMCs (P4) reached 80% or 100%, the DME/F12 complete medium was replaced with osteogenic or adipogenic induction medium (Cyagen, Guangzhou, China), and cultured for the appropriate time period according to the manufacturer's instructions. Alizarin Red S staining and Oil Red O staining kits (Cyagen, Guangzhou, China) were used to detect

the osteogenic and adipogenic differentiation potential of the hAMCs.

Myogenic differentiation of hAMCs induced by 5-Aza

hAMCs (P4) were seeded at a density of 5000/well in normal and gelatin methacryloyl hydrogel (GelMA gel) (Suzhou Intelligent Manufacturing Research Institute, China) embedded 24-well plates, and cultured in DME/F12 complete medium. Induction medium (DME/F12 complete medium containing 5-, 10-, or 50-μM 5-Aza (A2385, Sigma, USA)) was used to replace the DME/F12 complete medium after the cells had adhered to the plate. After 24 h of induction, the cells were washed twice with PBS and then cultured in DME/F12 complete medium.

The cytotoxicity of 5-Aza toward hAMCs was determined using a Cell Counting Kit 8 (CCK-8) (Beyotime, Shanghai, China). hAMCs were cultured in 96-well plates at a density of 2000/well in DME/F12 complete medium for 24 h. Induction medium containing different concentrations of 5-Aza (5, 10, and 50 μM) was added, and 24 h later, the medium was replaced with DME/F12 complete medium; cells not exposed to 5-Aza were used as a negative control group. Five repeated samples were obtained for each group. The absorbance at 450 nm of each sample was measured using a CCK-8 kit on days 1, 3, 5, and 7 after induction.

The cytotoxicity of the GelMA gel toward hAMCs was examined using live dead cell staining. hAMCs were seeded in 5% GelMA gel–embedded 24-well plates and cultured for 5 days in DME/F12 complete medium, and the cell viability was measured using a live dead cell staining kit (KA0901, Abnova, China) and observed using an inverted microscope.

The potential role of the Wnt/β-catenin signaling pathway in the 5-Aza-induced myogenic differentiation of hAMCs was examined. hAMCs treated with 10-μM 5-Aza induction medium were used as the induction group, and induction medium containing 30-μM ICG001 (S2662, Selleckchem, USA) was used for the negative control group to detect changes in the expression of Wnt/β-catenin signaling pathway–related proteins.

Western blot analysis

The cells were washed with precooled PBS, scraped and collected, and centrifuged. The cells were resuspended in radioimmunoprecipitation assay (RIPA) lysis buffer (Multi Sciences, Hangzhou, China) containing protease inhibitor, lysed on ice for 30 min, and centrifuged at 15,000 r/min at 4°C for 20 min. The supernatant was collected, and protein quantification was performed using an Enhanced Bicinchoninic Acid (BCA) Protein Assay Kit (Beyotime, Shanghai, China). Then, the sample was heated at 100°C for 5 min to denature the protein and stored at −80 C until use. Then, 20 μg of sample was loaded to perform 10% sodium dodecyl sulfate–polyacrylamide gel electrophoresis (SDS-PAGE), and the protein was transferred to a polyvinylidene fluoride membrane (Invitrogen, Carlsbad, USA), and incubated with rabbit anti-human desmin (ab32362, 1/100,000, Abcam, Cambridge, UK), rabbit anti-human MyoD (ab203383, 1/1000), mouse anti-human glycogen synthase kinase 3 β (GSK3β) (ab93926, 1/2000), rabbit anti-human phosphorylated s9 glycogen synthase kinase 3 β (ps9-GSK3β) (ab107166, 1/500), rabbit anti-human β-catenin (ab16051, 1/5000), or mouse anti-human glyceraldehyde 3-phosphate dehydrogenase (GAPDH) (ab8245, 1/10,000) antibody overnight at 4 C. A goat anti-rabbit or mouse horseradish peroxidase (HRP)-conjugated antibody (Multi Sciences, Hangzhou, China) was used as a secondary antibody, and incubated for 1 h at room temperature, and the bands were quantitatively analyzed using Image Lab software.

Immunofluorescence staining

The cells were washed twice with precooled PBS and fixed on ice for 4 min with 4% paraformaldehyde, followed by two washes with PBS for 5 min each. The cells were permeabilized with 0.1% Triton X-100 (Beyotime, Shanghai, China) for 10 min and washed twice with PBS. Thereafter, the cells were blocked with Quickblock blocking buffer (Beyotime, Shanghai, China) on ice for 1 h, and incubated with rabbit anti-human desmin (ab32362, 1/50), rabbit anti-human MyoD (ab203383, 1/200), and rabbit anti-human β-catenin (ab16051, 1/1000) antibodies overnight at 4°C. After removing excess antibody by washing three times with PBS, Alexa Fluor 488 goat anti-rabbit IgG (H + L) antibody (ab150077, 1/500) was used, and incubation was carried out for 1 h in the dark at 37°C, after which the nuclei were stained with 4′,6-diamidino-2-phenylindole (DAPI) stain for 5 min. After the staining was complete, the sample was observed using an inverted microscope or a confocal microscope.

Myogenic potential of hAMCs in vivo

Animal welfare and experimental procedures were carried out in accordance with the Declaration of Helsinke, and were approved by the Ethics Committee of the First Affiliated Hospital of Soochow University (approval number: 201805A008). According to the results of previous studies,[22] 6- to 8-week-old male Sprague Dawley (SD) rats (n = 32) were selected, and the tibialis anterior (TA) muscle in each was exposed. A 5-mm diameter muscle defect in the middle of the muscle was made using a hole punch. The rats were divided into four groups: (1) blank group (simple defect, n = 8), (2) GelMA group (5% GelMA, n = 8), (3) hAMCs group (5% GelMA + normal hAMCs,

cell density 500,000/mL, n = 8), and (4) 5-Aza group (5% GelMA + 10-μM 5-Aza induced hAMCs, cell density 500,000/mL, n = 8). GelMA gel with or without hAMCs was implanted into the defect area, and the group with the simple defect was used as a negative control. The TA muscle was harvested at 2 and 4 weeks after surgery, and paraffin-embedded sections were obtained.

Histological analysis

The TA muscles in the rats were harvested at 2 and 4 weeks after surgery, and the specimens were paraffin-embedded according to standard methods. In brief, the TA muscles were fixed in 4% paraformaldehyde for 24 h after harvest. After dehydration with an alcohol gradient, the specimen was embedded in a paraffin block using a paraffin-embedding machine. The paraffin block was serially sliced at a thickness of 6 μm using a microtome, and the sections were subjected to hematoxylin and eosin (H&E) and Masson trichrome staining. For the immunohistological analysis of vascular endothelial growth factor receptor 2 (VEGFR-2), the sections were incubated with rabbit anti-rat VEGFR-2 (ab2349, 1/100) overnight at 4°C. The sections were incubated with biotin-conjugated secondary antibodies for 30 min and then incubated with avidin–biotin reagent for 30 min at 37°C. Color development was carried out using 3,3′-diaminobenzidine tetrahydrochloride and hematoxylin as a counterstaining agent. Image acquisition was performed using an upright microscope.

Statistical analysis

Statistical analysis was performed using SPSS software. One-way analysis of variance (ANOVA) was utilized to perform multiple comparisons, and all data were expressed as the mean ± standard deviation (SD); a value of $p < 0.05$ indicated that there was a statistically significant difference between the groups.

Results

Morphological characteristics and proliferation of hAMCs

In this study, we collected five amniotic specimens and performed cell extraction according to the above-described method (Figure 1(a)). We observed that the hAMCs (P0) showed partial adherence 48 h after extraction, and 80% of adherent cells showed a spindle-like shape (Figure 1(b)), while the hAECs (P0) showed partial adherence at 24 h, and the cells showed a thin strip shape (Figure 1(c)). We changed the medium every 2 days. The hAMCs (P0) reached 90% density after 7 days of culture, while the hAECs (P0) reached only 50% density on the seventh day. It can be seen that the morphology and proliferative characteristics of the two cells are different. hAMCs can be separated from hAECs using the above cell extraction method. When the hAMCs density reached 90%, a 1/3 passage was performed. After passaging, the proliferation of the hAMCs accelerated and was similar to that of the hAMCs (P3); the number of cells doubled every 48 h, and the cell morphology showed a spindle-like shape. Better purity, and faster proliferation rate also, facilitates subsequent experiments and even clinical applications.

Multilineage identification of hAMCs

hAMCs (P4) were used for flow cytometry analysis and osteogenic and adipogenic differentiation. The flow cytometry results showed that most hAMCs expressed high levels of CD73, CD90, and CD105 and low levels of CD34, CD45, and HLA-DR (Figure 1(d)), and no significant differences were observed between all five cell samples, which is consistent with mesenchymal stem cell–specific surface marker standards[23]; so, we can term hAMCs as human amniotic mesenchymal stem cells too.

Calcium nodules were observed after 4 weeks of culture in osteogenic induction medium, and Alizarin Red S staining confirmed the differentiation of hAMCs into osteoblasts. After 4 weeks of culture in the adipogenic induction medium, many lipid droplets were observed in the hAMCs, and Oil Red O staining confirmed the differentiation of the hAMCs into adipocytes (Figure 1(e)). These results revealed the multilineage identification capacity of hAMCs.

Myogenic differentiation of hAMCs in vitro induced by 5-Aza

The results of the CCK-8 assay showed that on day 1, the absorbance of the samples induced with 5-, 10-, or 50-μM 5-Aza gradually decreased compared with that of samples in the normal group, and the difference was statistically significant, that is, the inhibition of cell growth was more pronounced as the concentration of 5-Aza was increased (Figure 2(a)); so, we controlled the intervention time of 5-Aza at 24 h. We performed western blot analysis of the hAMCs induced with different concentrations of 5-Aza (5, 10, and 50 μM) (Figure 2(b)). The expression of desmin and MyoD was significantly increased in the 5-Aza-treated group relative to that in the control group. Compared with that in the 5-μM 5-Aza treatment group, the expression of desmin and MyoD in the 10-μM 5-Aza treatment group was increased, and the difference was statistically significant, while there was no significant difference in their expression between the 10- and 50-μM 5-Aza treatment groups. Considering that the cytotoxicity of 5-Aza is positively correlated with the drug concentration, we took 10 μM of 5-Aza for subsequent animal experiments. In the 10-μM 5-Aza treatment group, the expression of desmin was increased on the seventh day compared with the first day,

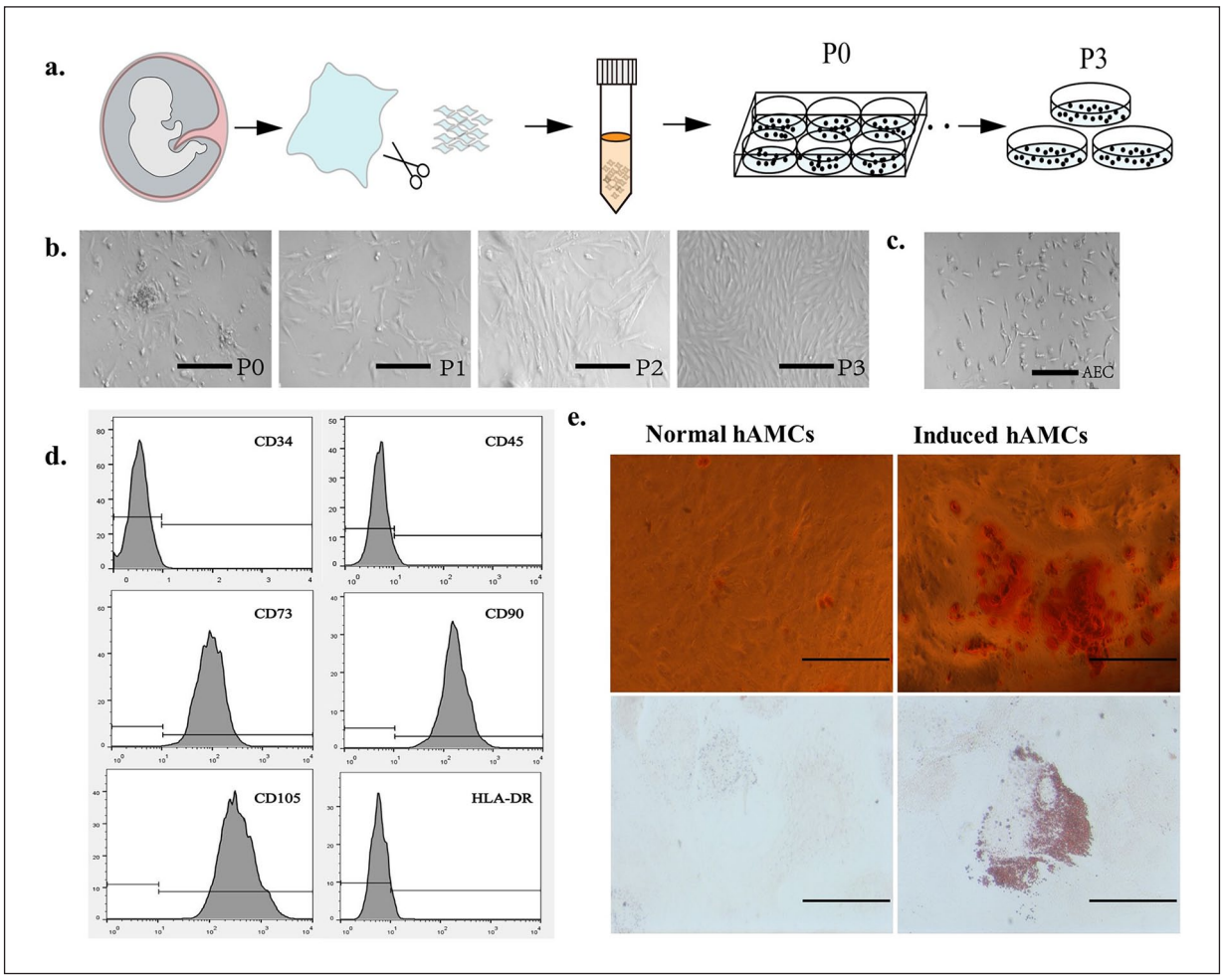

Figure 1. Extraction of hAMCs and its pluripotency. (a) Schematic diagram of hAMCs extraction from amniotic tissue. (b) Cell morphology of P0–P3 hAMCs, P0 cells were polymorphic, and P3 cells were spindle-like shape. Bar = 100 μm. (c) hAECs were thin strip shape. Bar = 100 μm. (d) Results of flow cytometry analysis of hAMCs, hAMCs expressed low levels of CD34, CD45, and HLA-DR, and highly expressed CD73, CD90, and CD105. (e) Alizarin Red S staining after 4-weeks osteogenic induction of hAMCs. Oil Red O staining results after 4-weeks adipogenic induction of hAMCs. Bar = 50 μm.

and the difference was statistically significant. Interestingly, this time-related increase in expression was not observed for MyoD. Immunofluorescence staining of desmin and MyoD was performed, and the results showed that the expression levels of desmin and MyoD were significantly increased compared with those in the control group (Figure 2(c)), which was also consistent with western blotting results. The results confirmed that hAMCs possess the capacity of myogenic differentiation in vitro.

The role of the Wnt/β-catenin signaling pathway in 5-Aza-induced hAMCs myogenic differentiation

The Wnt/β-catenin signaling pathway plays an important role in regulating cell proliferation and differentiation; thus, we investigated whether the Wnt/β-catenin signaling pathway participated in the 5-Aza-induced myogenic differentiation of hAMCs. The results showed (Figure 3(a)) that compared with the control group, the expression of GSK3β was decreased in the hAMCs subject to 5-Aza treatment, while the expression of ps9-GSK3β was increased, and the expression of GSK3β and ps9-GSK3β was correlated with the concentration of 5-Aza. The difference between the expression of GSK3β and ps9-GSK3β in 5-μM 5-Aza-treated hAMCs and the control group was not statistically significant, while the expression of GSK3β and ps9-GSK3β in the 10-μM 5-Aza treatment group was significantly higher than that in normal hAMCs. Interestingly, the difference between 50- and 10-μM 5-Aza-treated groups was not statistically significant. There was a positive correlation between the expression of β-catenin and the concentration of 5-Aza. We found that the expression of β-catenin was significantly increased in the 10-μM 5-Aza group compared with the control group, while there was no statistically significant difference in the

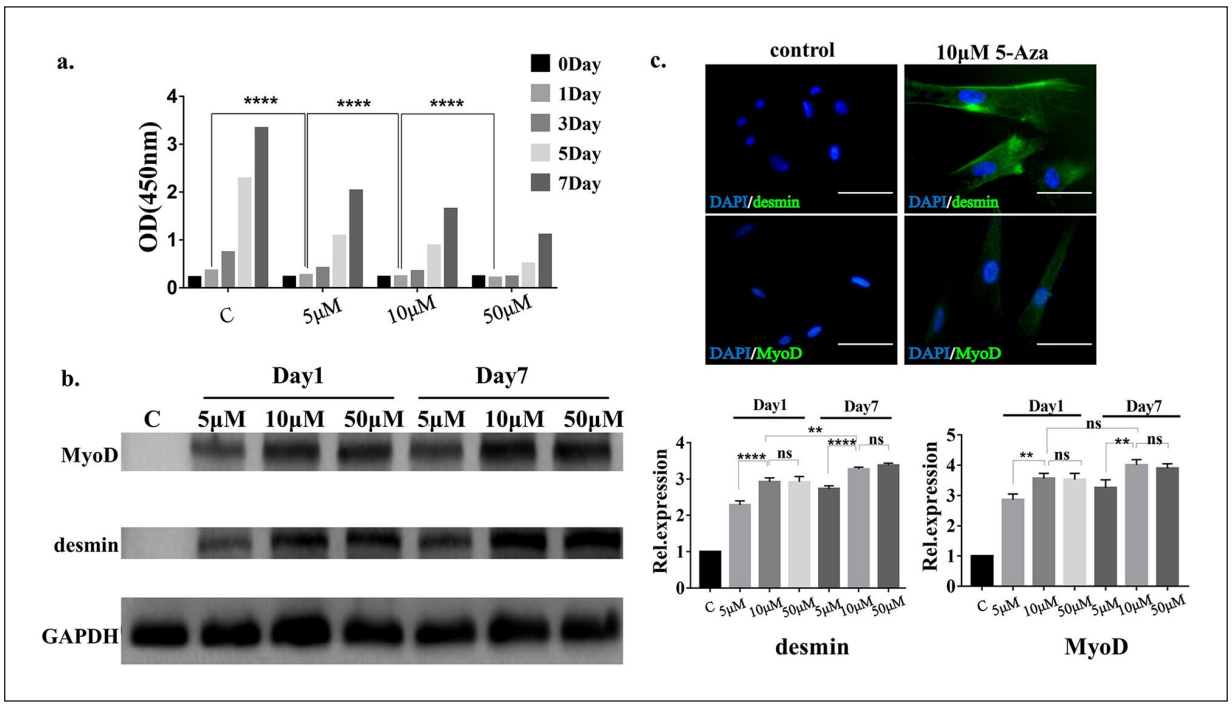

Figure 2. Cytotoxicity of 5-Aza and myogenic differentiation of hAMCs. (a) Effect on cell proliferation of hAMCs of different concentrations 5-Aza. After 24-h induction of hAMCs with 5-Aza, and the absorbance at wavelength of 450 nm was measured at 1, 3, 5, and 7 days after induction, the average value of five replicate samples was taken. ****$p < 0.0001$. (b) Western blot results of MyoD and desmin, and their semiquantitative results of hAMCs inducted by different concentrations 5-Aza. GAPDH is termed as an internal reference. The expression of MyoD and desmin was significantly increased in the 5-Aza treated group relative to that in the control group. **$p < 0.01$, ****$p < 0.0001$. (c) Immunofluorescence staining of desmin and MyoD of hAMCs, cells were inducted by 10-μM 5-Aza for 24 h. Bar = 50 μm.

expression of β-catenin in the 50-μM group compared with that in the 10-μM 5-Aza group.

We also examined changes in the myogenic differentiation of hAMCs treated with 5-Aza after suppression of the Wnt/β-catenin signaling pathway. The results showed (Figure 3(b)) that the expression of MyoD and desmin in hAMCs treated with 10 μM of 5-Aza was significantly decreased after the hAMCs were exposed to the Wnt/β-catenin signaling pathway–specific inhibitor ICG001. We also observed that ICG001 significantly decreased the expression of β-catenin, indicating that ICG001 is effective in inhibiting the Wnt/β-catenin signaling pathway. Immunofluorescence staining showed (Figure 3(c)) that 5-Aza induction significantly increased the expression of β-catenin in hAMCs, resulting in an increase in β-catenin entering the nucleus, and ICG001 inhibited this positive effect. According to these results, we believe that the Wnt/β-catenin signaling pathway participated in the regulation of myogenic differentiation of hAMCs induced by 5-Aza.

The effect of hAMCs on VML

To facilitate the colonization of hAMCs within the TA muscle defect, we used GelMA gel, which can be photocoagulated at room temperature and is very convenient to use, as a delivery vehicle for the cells (Figure 4(a)). We implanted the hAMCs in a 5% GelMA gel and observed that the hAMCs clustered into a block, and the cell morphology did not change significantly compared with that of normal hAMCs (Figure 4(b)). To detect the cytocompatibility of the GelMA gel, we performed live dead cell staining in hAMCs cultured on GelMA gel for 5 days; the results showed that cell viability was not significantly affected (Figure 4(c)), and the results of the immunofluorescence staining of desmin and MyoD (Figure 4(d)) showed that the induction of the myogenic differentiation of hAMCs by 5-Aza was not affected by GelMA gel.

H&E and Masson trichrome staining showed (Figure 5) that at 2 weeks, the blank group lesions were filled with disordered scar tissue in the defect area. At 4 weeks, there was still no obvious muscle repair present in the defect area. In the GelMA group, at 2 weeks, H&E staining showed the partial degradation of the GelMA gel in the defect area, and there was no obvious muscle fiber regeneration inside the defect area; the degradation of the GelMA gel was increased at 4 weeks, and no regenerated muscle fibers were observed. Masson trichrome staining showed that many inflammatory cells infiltrated into the defect area at the margin of the defect, and no muscle

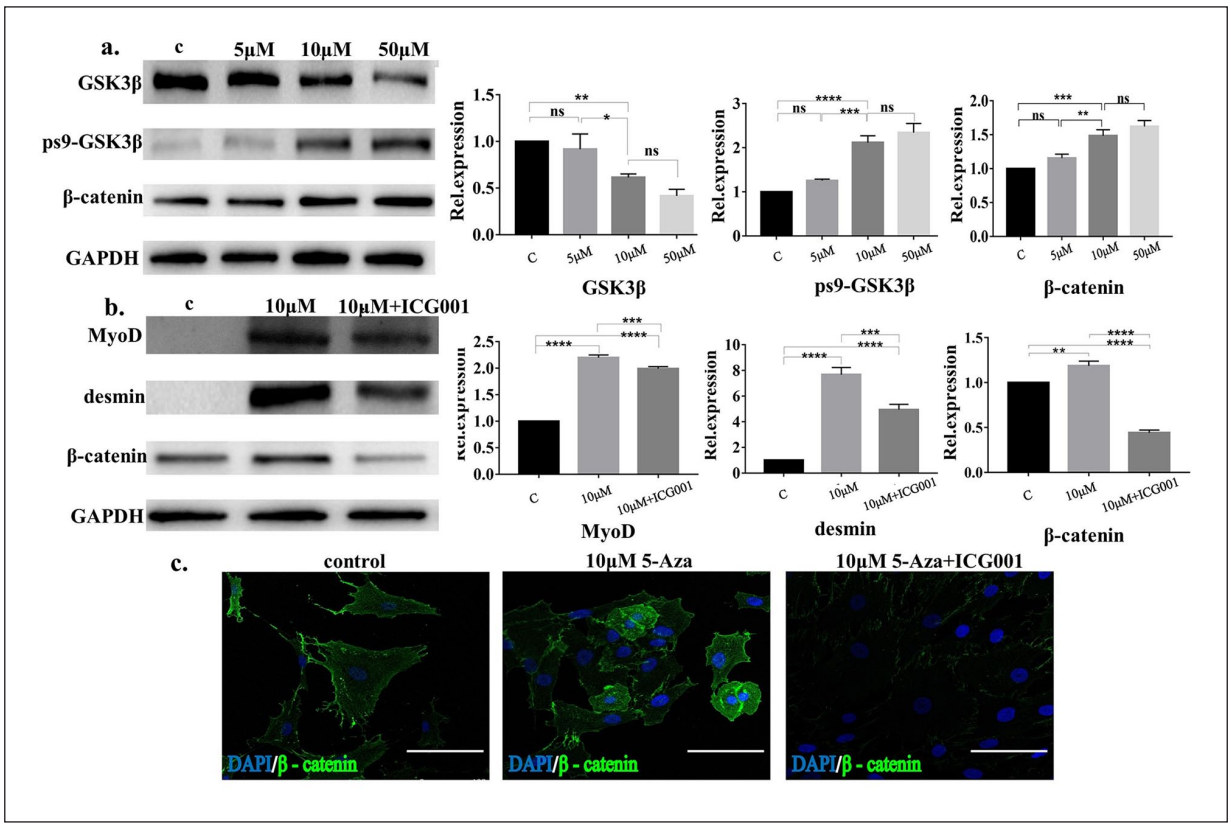

Figure 3. Myogenic differentiation of hAMCs induced by 5-Aza was associated with the activation of the Wnt/β-catenin signaling pathway. (a) Western blot results of GSK3β, ps9-GSK3β, and β-catenin and their semiquantitative results of hAMCs inducted with different concentrations 5-Aza for 24 h, GAPDH was termed as an internal reference. *$p < 0.05$, **$p < 0.01$, ***$p < 0.001$, ****$p < 0.0001$. (b) Western blot results of MyoD, desmin, and β-catenin and their semiquantitative results after 24-h induction of hAMCs with 10-μM 5-Aza or with ICG001 inhibitor, GAPDH was termed as an internal reference. (c) Immunofluorescence of β-catenin of hAMCs, cells were inducted by 10-μM 5-Aza or with ICG001 for 24 h. Bar = 50 μm.

fibers appeared in the defect area. In the hAMCs group, the histological results showed that there was agglomeration of cells in the defect area at 2 weeks, and some cells showed signs of fusion, a few signs of angiogenesis were observed in the marginal area of the defect. In the 5-Aza group, we observed increased neovascularization at the edge of the defect, and more cells were fused together, there was little multi-nucleation fiber-like tissue around the area of neovascularization. The results of immunohistochemistry showed (Figure 6(a)) that in the blank group and the GelMA group, no neovascularization was observed in the defect area adjacent to the normal tissue, and in the hAMCs group, VEGFR-2-positive blood vessels were observed 2 and 4 weeks after implantation, but the increase in the number of blood vessels was not statistically significant (Figure 6(b)). In the 5-Aza group, more VEGFR-2-positive blood vessels were observed at 2 weeks, and the number of blood vessels was significantly increased at 4 weeks. The difference in the number of VEGFR-2 positive vessels between the 5-Aza group and the hAMCs group was statistically significant (Figure 6(b)); in other words, 5-Aza-induced hAMCs have shown the strongest angiogenesis. In conclusion, the 5-Aza group showed the best histological performance.

Discussion

Human amniotic tissue is an attractive source of stem cells for tissue engineering and regenerative medicine. First, hAMCs are easily obtained from cesarean sections in a way that is harmless to pregnant women and fetuses, and placental tissue is often treated as medical waste, in other words, eliminate ethical issues. Second, hAMCs can be expanded in vitro and exhibit the characteristics of mesenchymal stem cells. Our research also confirmed their multidirectional differentiation potential. Finally, the amniotic membrane, as a natural barrier between the fetus and the mother, has low immunogenicity, excellent anti-inflammatory and anti-microbial properties,[24,25] and a proliferation rate that is lower than that of other stem cells[26]; so, its tumorigenicity is decreased. The amniotic membrane has been widely used in skin repair[27] and ophthalmology[28,29] in previous studies, and it has been used to improve the repair of tendon injuries[30,31]; however, whether

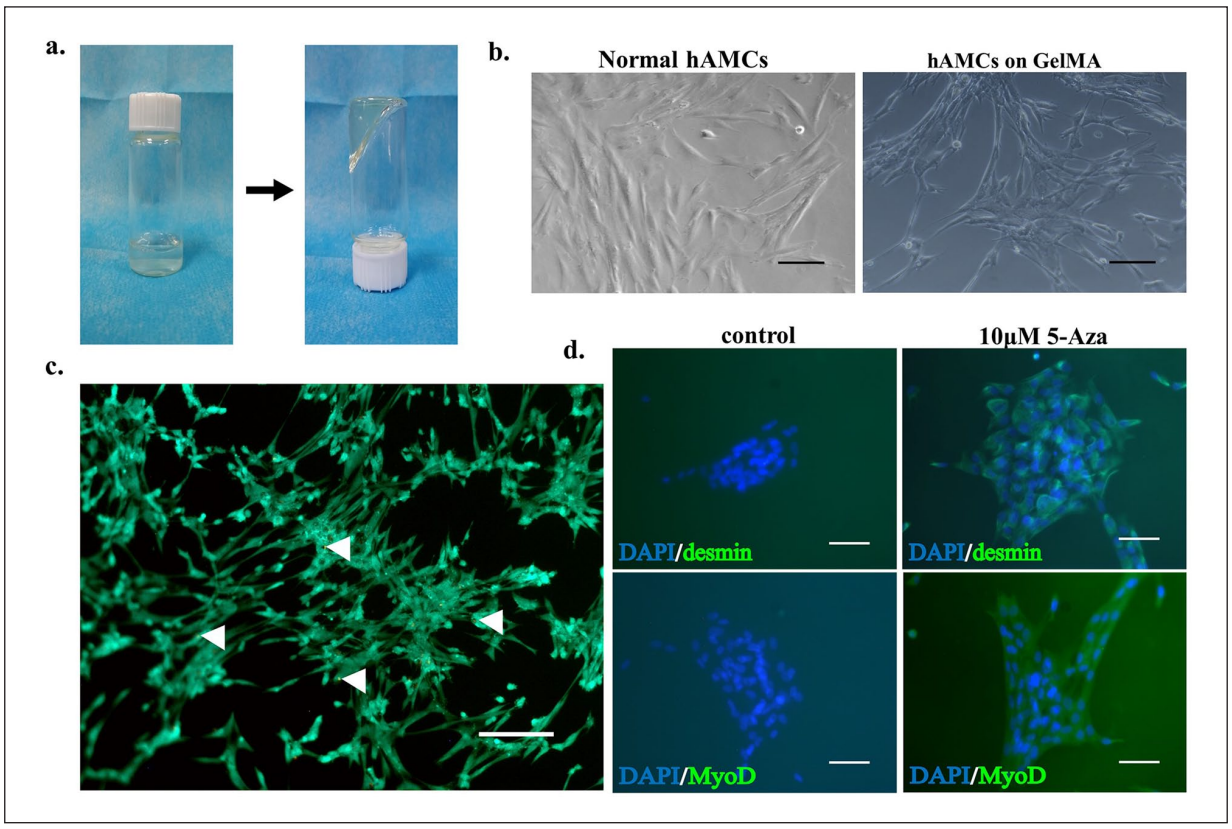

Figure 4. Effect on hAMCs' morphology and myogenic differentiation of GelMA gel. (a) Photocoagulation characteristics of GelMA gel at room temperature. (b) hAMCs (P3) cultured on common culture dish and GelMA gel, no significantly difference of cell morphology was observed compared with that of normal hAMCs. Bar = 50 μm. (c) Live dead cell staining of hAMCs cultured on GelMA gel for 5 days, white arrows indicate dead cells, cellular activity was not affected by GelMA gel significantly. Bar = 50 μm. (d) Immunofluorescence staining of desmin and MyoD of hAMCs, cells were inducted by 10-μM 5-Aza on GelMA gel for 24 h. Bar = 100 μm.

it could be used in skeletal muscle remained unclear. We hypothesized that amniotic cells may be a promising cell source for cell therapies for VML.

The amniotic membrane is located on the innermost surface of placental tissue and can be divided into an epithelial layer and an interstitial layer that are on the fetal side and the maternal side, respectively. The interstitial layer can be subdivided into the basement membrane, compact layer, fibroblast layer, and spongy layer.[32] As shown by the flow cytometry analysis results, the low expression of HLA-DR also explains the low immunogenicity of amniotic tissue to some extent. Moreover, CD90 antigen expression shows a certain relationship with the cell growth rate, and flow cytometry analysis showed that most of the hAMCs expressed CD90, which is consistent with previous findings.[33–35] The capability in vitro osteogenesis and adipogenic differentiation further confirmed the pluripotency of the hAMCs, and according to the above experimental results, we believe that hAMCs are a promising cell source for tissue engineering. Therefore, in this study, we used hAMCs as a source of cells for VML cell therapies.

Our study confirmed the myogenic differentiation potential of hAMCs for the first time. According to previous studies, 5-Aza can induce myogenic differentiation of pluripotent stem cells by inhibiting methylation of DNA. We found that hAMCs can express myogenic cell–specific protein desmin and Myod under the induction of 5-Aza in vitro. Previous studies have demonstrated that during the regeneration of muscle tissue, the activation of the Wnt/β-catenin signaling pathway in myoblasts is enhanced and is necessary for commitment to final differentiation.[36,37] Rudolf et al.[38] also found that the Wnt/β-catenin signaling pathway is essential for maintaining the function of satellite cells, and the loss of β-catenin function leads to defects in muscle regeneration. Therefore, we hypothesized that the Wnt/β-catenin signaling pathway also plays an important role in the myogenic differentiation of hAMCs. Western blotting and immunofluorescence results showed that the activation of the Wnt/β-catenin signaling pathway in hAMCs was significantly up-regulated after 5-Aza treatment compared with that in the control group, and the expression of desmin and MyoD decreased significantly after using the Wnt/β-catenin signaling pathway–specific

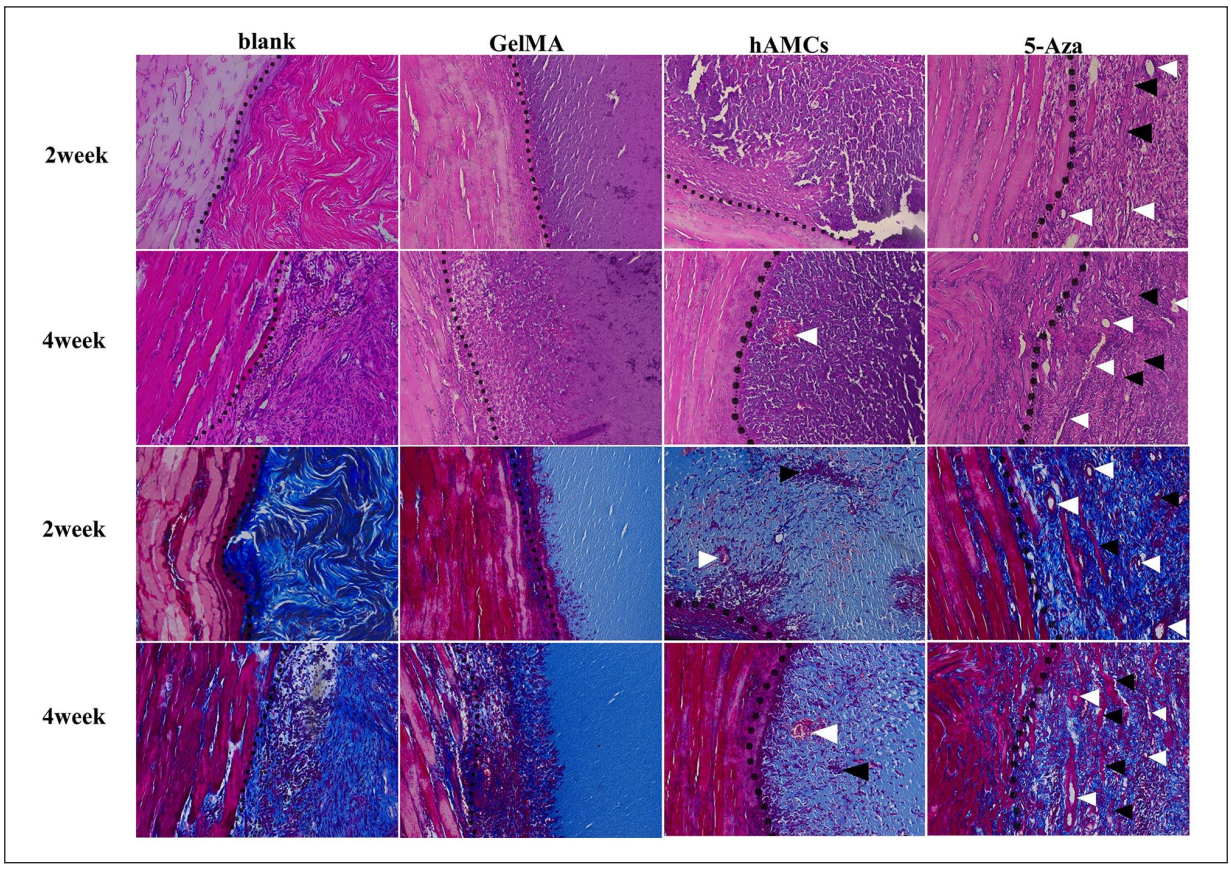

Figure 5. hAMCs improved tissue repair on VML. H&E and Masson trichrome staining of 2 and 4 weeks after establishment of VML model (blank group), implantation of GelMA gel (GelMA group), GelMA + hAMCs (hAMCs group), and GelMA + 5-Aza-inducted hAMCs (5-Aza group). The dotted line is the boundary between normal muscle tissue and defect. White arrow shows the neovascularization, black arrow shows fused hAMCs and fiber-like tissue. 200×.

inhibitor ICG001. According to the above experimental results, we believe that the activation of the Wnt/β-catenin signaling pathway plays an important role in the myogenic differentiation of hAMCs induced by 5-Aza.

To verify whether the myogenic differentiation ability of hAMCs can improve skeletal muscle tissue repair after VML, we implanted hAMCs into the TA muscle of rats. The establishment of animal models of VML is important for determining the effects of the implantation of hAMCs. It is well known that when skeletal muscle is damaged, satellite cells migrate to the damaged area, differentiate, and fuse into muscle fibers to repair muscle damage. When VML occurs, the large muscle mass loss is accompanied by the loss of satellite cells, basement membrane, blood vessels, and nerves, and a strong inflammatory response can further hinder the repair of the injury. The outcome is often a large amount of fibrous scar deposition in the injured area and the loss of muscle function. We used 6- to 8-week-old SD male rats as experimental animals. The TA muscle was perforated with a puncher to form a skeletal muscle defect with a defect volume comprising approximately 30% of the TA muscle. Histological observation of the TA muscle at 2 and 4 weeks after surgery showed that scar deposition occurred in the defect area, and no obvious muscle tissue regeneration was observed, indicating the successful establishment of the VML animal model.

To facilitate colonization of implanted cells in the defect area and prevent cell loss, the use of cell carriers was particularly necessary. Hydrogels are widely used as biomaterials in the study of skeletal muscle tissue engineering.[39,40] GelMA gel is a light-cured gel that is also widely used in tissue engineering.[41,42] Microscopic observation and live dead cell staining showed that there were no significant differences in the morphology and cell survival rate of cells cultured on GelMA gel compared with those of normal hAMCs, indicating that the cell compatibility of the GelMA gel was excellent. The immunofluorescence results further confirmed that the GelMA gel did not significantly affect the myogenic differentiation of hAMCs. Therefore, we believe that GelMA gel is a safe and convenient cell carrier. Grzywocz et al.[43] found that hAMCs secreted fibroblast growth factor 6 and vascular endothelial growth factor receptor 3. Wu et al.[44] also found that hAMCs expressed basic fibroblast growth factor and hepatocyte growth factor

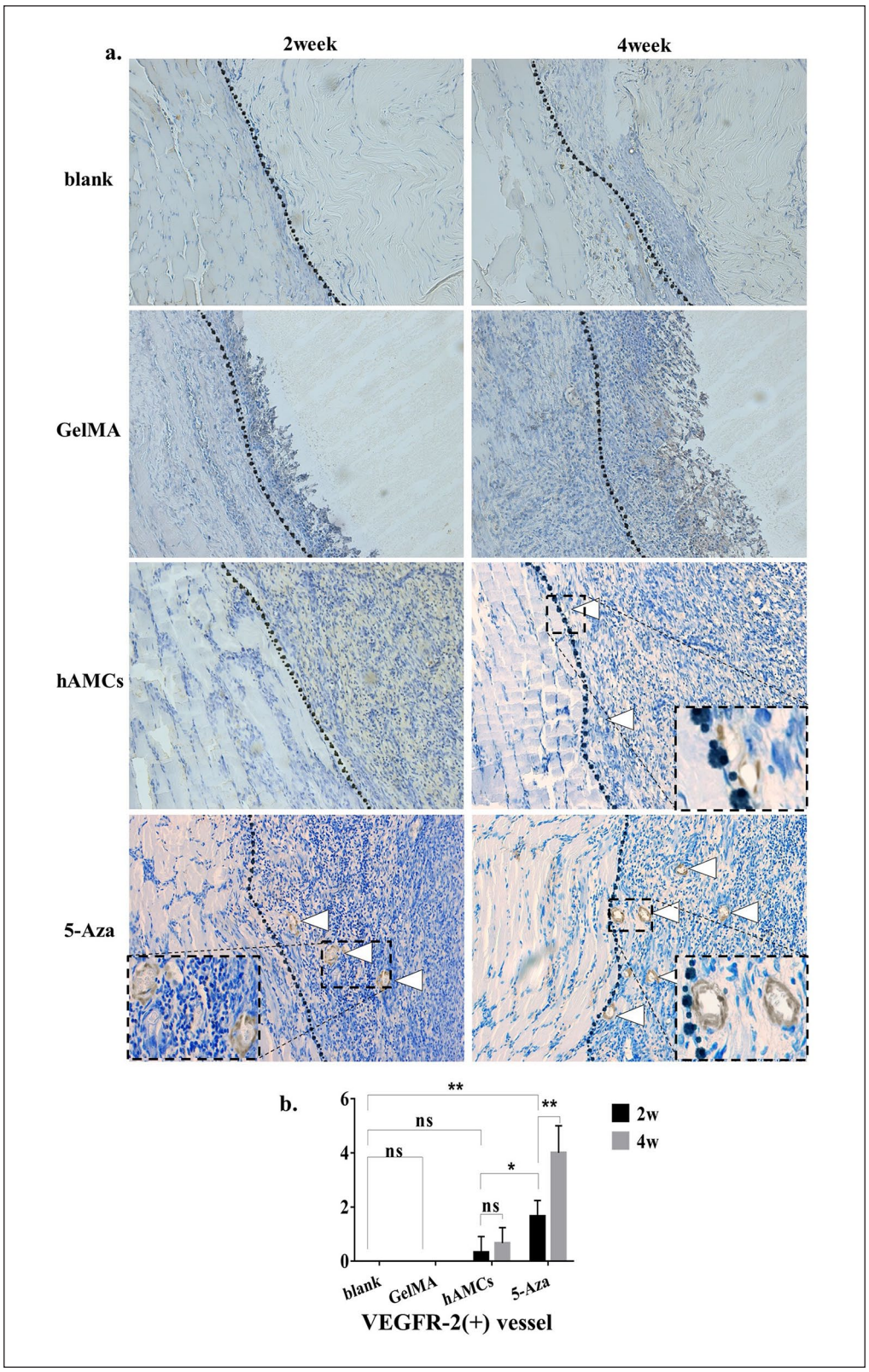

Figure 6. hAMCs induced neovascularization on VML. (a) Immunohistochemical staining results of VEGFR-2 in the defect area at 2 and 4 weeks after establishment of VML model (blank group), implantation of GelMA gel (GelMA group), GelMA + hAMCs (hAMCs group), and GelMA + 5-Aza-inducted hAMCs (5-Aza group). The dashed box shows partially enlarged image of the neovascularization. The dotted line is the boundary between normal muscle tissue and defect. White arrow shows the neovascularization. 200×. (b) Semiquantitative analysis of the number of VEGFR-2 positive blood vessels. *$p < 0.05$, **$p < 0.01$.

(HGF), which promoted vascular endothelial cell proliferation and angiogenesis. Moreover, HGF is considered to be a driver of satellite cell activation and proliferation, and it is important for the migration of myogenic precursor cells to damaged areas.[45,46] In vivo, we found that 2 weeks after implantation, there were only a few new blood vessels at the edge of the defect in the hAMCs group. This phenomenon was not observed in the blank group or the GelMA group. However, the histological performance of 5-Aza-induced hAMCs was encouraging. Two weeks after implantation, we observed increased neovascularization, similar to that observed by Pilia et al.[6] when using microvascular fragments implanted into the rat TA muscle, indicating that 5-Aza-induced hAMCs have stronger angiogenic capability. Prior to this, Kesireddy[47] observed the fusion of cells and the formation of elongated fibers after the implantation of rat ADSCs combined with urinary bladder acellular scaffolds after rat VML injury. We obtained similar results using hAMCs in combination with GelMA gels, without the need for in vitro preculture; we found that cell fusion occurred in the hAMCs group 2 weeks after implantation, while more hAMCs were fused and more fiber-like tissue was found in the defect area near normal muscle tissue in the 5-Aza group, indicating that this could improve local tissue repair. The successful repair of skeletal muscle injury requires not only the proliferation and fusion of myoblasts but also the regeneration of blood vessels. The ability of hAMCs to induce angiogenesis and to fuse with each other will play an active role in repairing skeletal muscle defects.

Conclusion

In conclusion, our results show that hAMCs have the characteristics of pluripotent stem cells and can differentiate into myoblasts. The activation of the Wnt/β-catenin pathway may play an important role in the myogenic differentiation of hAMCs induced by 5-Aza. Moreover, after pretreatment with 5-Aza, the hAMCs showed improved histological performance after VML and increased angiogenesis in the injured area. However, the treatment of VML is not limited to improving tissue repair, and functional improvement is also crucial; therefore, future research will need to consider the effects of different therapies on muscle function. Based on the above findings and advantages on ethical issue, we believe that hAMCs can serve as a potential source of cells for skeletal muscle tissue engineering.

Acknowledgements

I would like to express my gratitude to Dr. Xiaojun Zou and Dr. Jianping Qiu, sincerely thank the Department of Obstetrics and Gynecology of the North District of The Affiliated Suzhou Hospital of Nanjing Medical University for its selfless help.

Author contributions

W.B.S., Y.F.H., D.C.G., and D.Z. conceived and designed the research. K.Y., J.Z., T.P.X., M.L.X., and D.Z. performed the experiments, collected data, and conducted research. J.Y.L., J.X.B., G.R.G., and D.H. analyzed and interpreted data. D.Z. wrote the initial manuscript. W.B.S., Y.F.H., D.C.G., and D.Z. revised the manuscript. W.B.S. was primarily responsible for the final content. All authors have reviewed and approved the final manuscript.

Declaration of conflicting interests

The author(s) declared no potential conflicts of interest with respect to the research, authorship, and/or publication of this article.

Funding

The author(s) disclosed receipt of the following financial support for the research, authorship, and/or publication of this article: This research was supported by the Program for Introduction of Clinical Medical Teams to Suzhou (grant no.: SZYJTD201714), Program from Jiangsu Health and Health Committee (grant no.: H2018027), and Social Development Program from Suzhou Science and Technology Bureau (grant no.: SYSD2017170, SS201805, and SYSD2018207). The PICMTS provided location for experiments and animal feeding. All of these funding supported the design of study, collection, analysis, and interpretation of data, and final writing of the manuscript.

ORCID iD

Di Zhang https://orcid.org/0000-0002-1317-9535

Data sharing and accessibility

The datasets used and analyzed during the current study are available from the corresponding author on reasonable request.

Supplemental material

Supplemental material for this article is available online.

References

1. Garg K, Ward CL, Hurtgen BJ, et al. Volumetric muscle loss: persistent functional deficits beyond frank loss of tissue. *J Orthop Res* 2015; 33(1): 40–46.
2. Greising SM, Rivera JC, Goldman SM, et al. Unwavering pathobiology of volumetric muscle loss injury. *Sci Rep* 2017; 7(1): 13179.
3. Ward CL, Pollot BE, Goldman SM, et al. Autologous minced muscle grafts improve muscle strength in a porcine model of volumetric muscle loss injury. *J Orthop Trauma* 2016; 30(12): e396–e403.
4. Hurtgen BJ, Ward CL, Leopold Wager CM, et al. Autologous minced muscle grafts improve endogenous fracture healing and muscle strength after musculoskeletal trauma. *Physiol Rep* 2017; 5(14): e13362.
5. Li MT, Ruehle MA, Stevens HY, et al. Skeletal myoblast-seeded vascularized tissue scaffolds in the treatment of a large volumetric muscle defect in the rat biceps femoris muscle. *Tissue Eng Part A* 2017; 23(17–18): 989–1000.
6. Pilia M, McDaniel JS, Guda T, et al. Transplantation and perfusion of microvascular fragments in a rodent model of volumetric muscle loss injury. *Eur Cell Mater* 2014; 28: 11–23.

7. Aurora A, Roe JL, Corona BT, et al. An acellular biologic scaffold does not regenerate appreciable de novo muscle tissue in rat models of volumetric muscle loss injury. *Biomaterials* 2015; 67: 393–407.
8. Corona BT, Wu X, Ward CL, et al. The promotion of a functional fibrosis in skeletal muscle with volumetric muscle loss injury following the transplantation of muscle-ECM. *Biomaterials* 2013; 34(13): 3324–3335.
9. Quarta M, Cromie M, Chacon R, et al. Bioengineered constructs combined with exercise enhance stem cell-mediated treatment of volumetric muscle loss. *Nat Commun* 2017; 8: 15613.
10. Huang H, Liu J, Hao H, et al. Preferred M2 polarization by ASC-based hydrogel accelerated angiogenesis and myogenesis in volumetric muscle loss rats. *Stem Cells Int* 2017; 2017: 2896874.
11. Aurora A, Wrice N, Walters TJ, et al. A PEGylated platelet free plasma hydrogel based composite scaffold enables stable vascularization and targeted cell delivery for volumetric muscle loss. *Acta Biomater* 2018; 65: 150–162.
12. Teng Z, Yoshida T, Okabe M, et al. Establishment of immortalized human amniotic mesenchymal stem cells. *Cell Transplant* 2013; 22(2): 267–278.
13. Toda A, Okabe M, Yoshida T, et al. The potential of amniotic membrane/amnion-derived cells for regeneration of various tissues. *J Pharmacol Sci* 2007; 105(3): 215–228.
14. Ranzoni AM, Corcelli M, Hau KL, et al. Counteracting bone fragility with human amniotic mesenchymal stem cells. *Sci Rep* 2016; 6: 39656.
15. Muinos-Lopez E, Hermida-Gomez T, Fuentes-Boquete I, et al. Human amniotic mesenchymal stromal cells as favorable source for cartilage repair. *Tissue Eng Part A* 2017; 23(17–18): 901–912.
16. Li Y, Liu Z, Jin Y, et al. Differentiation of human amniotic mesenchymal stem cells into human anterior cruciate ligament fibroblast cells by in vitro coculture. *Biomed Res Int* 2017; 2017: 7360354.
17. Kharat A, Chandravanshi B, Gadre S, et al. IGF-1 and somatocrinin trigger islet differentiation in human amniotic membrane derived mesenchymal stem cells. *Life Sci* 2019; 216: 287–294.
18. Hupkes M, Jonsson MK, Scheenen WJ, et al. Epigenetics: DNA demethylation promotes skeletal myotube maturation. *FASEB J* 2011; 25(11): 3861–3872.
19. Montesano A, Luzi L, Senesi P, et al. Modulation of cell cycle progression by 5-azacytidine is associated with early myogenesis induction in murine myoblasts. *Int J Biol Sci* 2013; 9(4): 391–402.
20. Ma X, Zhang S, Zhou J, et al. Clone-derived human AF-amniotic fluid stem cells are capable of skeletal myogenic differentiation in vitro and in vivo. *J Tissue Eng Regen Med* 2012; 6(8): 598–613.
21. Helinska A, Krupa M, Archacka K, et al. Myogenic potential of mouse embryonic stem cells lacking functional Pax7 tested in vitro by 5-azacitidine treatment and in vivo in regenerating skeletal muscle. *Eur J Cell Biol* 2017; 96(1): 47–60.
22. Pollot BE and Corona BT. Volumetric muscle loss. *Methods Mol Biol* 2016; 1460: 19–31.
23. Dominici M, Le Blanc K, Mueller I, et al. Minimal criteria for defining multipotent mesenchymal stromal cells. *Cytotherapy* 2006; 8(4): 315–317.
24. King AE, Paltoo A, Kelly RW, et al. Expression of natural antimicrobials by human placenta and fetal membranes. *Placenta* 2007; 28(2–3): 161–169.
25. Mamede AC, Carvalho MJ, Abrantes AM, et al. Amniotic membrane: from structure and functions to clinical applications. *Cell Tissue Res* 2012; 349(2): 447–458.
26. Kwon A, Kim Y, Kim M, et al. Tissue-specific differentiation potency of mesenchymal stromal cells from perinatal tissues. *Sci Rep* 2016; 6: 23544.
27. Farhadihosseinabadi B, Farahani M, Tayebi T, et al. Amniotic membrane and its epithelial and mesenchymal stem cells as an appropriate source for skin tissue engineering and regenerative medicine. *Artif Cells Nanomed Biotechnol* 2018; 46: 431–440.
28. Jirsova K and Jones GLA. Amniotic membrane in ophthalmology: properties, preparation, storage and indications for grafting: a review. *Cell Tissue Bank* 2017; 18(2): 193–204.
29. Rock T, Bartz-Schmidt KU, Landenberger J, et al. Amniotic membrane transplantation in reconstructive and regenerative ophthalmology. *Ann Transplant* 2018; 23: 160–165.
30. Leppanen OV, Karjalainen T, Goransson H, et al. Outcomes after flexor tendon repair combined with the application of human amniotic membrane allograft. *J Hand Surg Am* 2017; 42(6): 474.e1–474.e8.
31. Nicodemo MC, Neves LR, Aguiar JC, et al. Amniotic membrane as an option for treatment of acute Achilles tendon injury in rats. *Acta Cir Bras* 2017; 32(2): 125–139.
32. Niknejad H, Peirovi H, Jorjani M, et al. Properties of the amniotic membrane for potential use in tissue engineering. *Eur Cell Mater* 2008; 15: 88–99.
33. Yamahara K, Harada K, Ohshima M, et al. Comparison of angiogenic, cytoprotective, and immunosuppressive properties of human amnion- and chorion-derived mesenchymal stem cells. *PLoS ONE* 2014; 9(2): e88319.
34. Magatti M, Pianta S, Silini A, et al. Isolation, culture, and phenotypic characterization of mesenchymal stromal cells from the amniotic membrane of the human term placenta. *Methods Mol Biol* 2016; 1416: 233–244.
35. Afsartala Z, Rezvanfar MA, Hodjat M, et al. Amniotic membrane mesenchymal stem cells can differentiate into germ cells in vitro. *In Vitro Cell Dev Biol Anim* 2016; 52(10): 1060–1071.
36. Brack AS, Conboy IM, Conboy MJ, et al. A temporal switch from notch to Wnt signaling in muscle stem cells is necessary for normal adult myogenesis. *Cell Stem Cell* 2008; 2(1): 50–59.
37. Zhuang L, Hulin JA, Gromova A, et al. Barx2 and Pax7 have antagonistic functions in regulation of Wnt signaling and satellite cell differentiation. *Stem Cells* 2014; 32(6): 1661–1673.
38. Rudolf A, Schirwis E, Giordani L, et al. β-Catenin activation in muscle progenitor cells regulates tissue repair. *Cell Rep* 2016; 15(6): 1277–1290.
39. Pollot BE, Rathbone CR, Wenke JC, et al. Natural polymeric hydrogel evaluation for skeletal muscle tissue engineering. *J Biomed Mater Res B Appl Biomater* 2018; 106(2): 672–679.
40. Lev R and Seliktar D. Hydrogel biomaterials and their therapeutic potential for muscle injuries and muscular dystrophies. *J R Soc Interface* 2018; 15(138): 20170380.

41. Trujillo-de Yue K, Santiago G, Alvarez MM, et al. Synthesis, properties, and biomedical applications of gelatin methacryloyl (GelMA) hydrogels. *Biomaterials* 2015; 73: 254–271.
42. Xiao S, Zhao T, Wang J, et al. Gelatin methacrylate (GelMA)-based hydrogels for cell transplantation: an effective strategy for tissue engineering. *Stem Cell Rev Rep* 2019; 15(5): 664–679.
43. Grzywocz Z, Pius-Sadowska E, Klos P, et al. Growth factors and their receptors derived from human amniotic cells in vitro. *Folia Histochem Cytobiol* 2014; 52(3): 163–170.
44. Wu Q, Fang T, Lang H, et al. Comparison of the proliferation, migration and angiogenic properties of human amniotic epithelial and mesenchymal stem cells and their effects on endothelial cells. *Int J Mol Med* 2017; 39(4): 918–926.
45. Cezar CA and Mooney DJ. Biomaterial-based delivery for skeletal muscle repair. *Adv Drug Deliv Rev* 2015; 84: 188–197.
46. Grasman JM, Do DM, Page RL, et al. Rapid release of growth factors regenerates force output in volumetric muscle loss injuries. *Biomaterials* 2015; 72: 49–60.
47. Kesireddy V. Evaluation of adipose-derived stem cells for tissue-engineered muscle repair construct-mediated repair of a murine model of volumetric muscle loss injury. *Int J Nanomedicine* 2016; 11: 1461–1473.